

Cosmic-ray acceleration in a supernova remnant shock propagating in a stellar wind with a wind termination shock

Shoma F. Kamijima^{a,*} and Yutaka Ohira^b

^a*Yukawa Institute for Theoretical Physics, Kyoto University,
Oiwake-cho, Sakyo-ku, Kyoto-city, Kyoto, 606-8502, Japan*

^b*Department of Earth and Planetary Science, The University of Tokyo,
7-3-1 Hongo, Bunkyo-ku, Tokyo 113-0033, Japan*

E-mail: shoma.kamijima@yukawa.kyoto-u.ac.jp, y.ohira@eps.s.u-tokyo.ac.jp

We investigate the acceleration process of particles in core-collapse supernova remnants (SNRs) propagating in the circumstellar medium with the Parker-spiral magnetic field, current sheet, and wind termination shock (WTS). Wolf-Rayet (WR) stars are considered in this work as progenitors of supernovae. Test particle simulations are performed to reveal the particle motion between the SNR shock and WTS and attainable maximum energy without magnetic field amplification in the upstream region, where the magnetic field strength and rotation period expected from observations of WR stars are used. We show that particles can experience the cyclic motion between the SNR shock and WTS until the SNR shock collides with the WTS. Particles are accelerated at the SNR shock and WTS again and again and the attainable maximum energy can exceed the maximum energy limited by escape from core-collapse SNRs.

38th International Cosmic Ray Conference (ICRC2023)
26 July - 3 August, 2023
Nagoya, Japan



*Speaker

1. Introduction

Supernova remnants (SNRs) are believed to be the origin of Galactic cosmic rays (CRs). In addition to the spectral break around 3 PeV, recent observations reported that the energy spectrum of CR protons and heliums has the spectral break around 10 TeV [1]. Although 3 PeV is thought to be the maximum energy scale of Galactic CRs, it is still unclear what the energy scale about 10 TeV means. Diffusive shock acceleration (DSA) is the plausible acceleration mechanism to accelerate CRs up to the PeV scales [2]. In particular, the DSA at perpendicular shocks, where the magnetic field is perpendicular to the shock normal direction, can accelerate particles to the PeV scale without magnetic field amplification in the shock upstream region. Rapid perpendicular shock acceleration is confirmed by numerical simulations [3, 4].

Recent work show that the maximum energy of particles can be limited by escape from accelerators [5]. Our recent work investigated the escape process and maximum energy limited by escape from core-collapse SNRs propagating in the circumstellar medium with the Parker-spiral magnetic field and current sheet [6]. Not only the Parker-spiral magnetic field and current sheet but also the wind termination shock (WTS) created by the stellar wind of progenitors of core-collapse supernovae could realize in the circumstellar medium. Therefore, particles escaped from core-collapse SNRs eventually can interact with the WTS and could be accelerated again at the WTS. However, the particle motion between the SNR shock and WTS and attainable particle energy are still unclear.

In this work, we investigate CR acceleration and attainable energy in the core-collapse SNR shock propagating in the circumstellar medium with Parker-spiral magnetic field, current sheet, and WTS by using test particle simulations. As for the Parker-spiral magnetic field, the toroidal component can be larger than the radial component (see Equations (2) and (3)). Thus, most shock surfaces of the core-collapse SNR and WTS can be perpendicular shocks. In this work, the core-collapse SNR shock collides with WTS at about 1500 yr after the supernova explosion.

2. Simulation setup

This work focuses on core-collapse SNRs propagating in the free wind region (shock upstream region) until the SNR shock collides with the WTS. Test particle simulations are performed to investigate the particle motion between the SNR shock and WTS and attainable maximum energy in this system. Here, we consider high-energy protons. Particles with 100 GeV are impulsively injected on the SNR shock surface at the simulation start time. Wolf-Rayet (WR) stars, which are thought to be progenitor of type Ib/Ic supernovae, are considered as progenitors. We use observed values as parameters of WR stars. The surface magnetic field strength, B_* , stellar radius, R_* , mass loss rate, \dot{M} , and wind velocity, V_w , are set to be 100 G, $10R_\odot$, $10^{-4}M_\odot/\text{yr}$, and 3000 km/s, respectively. The time evolution of the SNR shock until the SNR shock collides with the WTS (≈ 1500 yr) is

$$u_{\text{SNR}}(t) = \frac{7}{8} \left[\frac{1}{10} \left(\frac{50}{21} \right)^{7/2} \frac{E_{\text{SN}}^{7/2} V_w}{M_{\text{ej}}^{5/2} \dot{M}} \right]^{1/8} t^{-1/8}, \quad (1)$$

where the wind density profile ($\rho_w = \dot{M}/(4\pi V_w r^2)$) and ejecta profile are assumed [7]. The explosion energy, E_{SN} , and ejecta mass, M_{ej} , are set to be 10^{51} erg and $5M_{\odot}$, respectively. $R_{\text{SNR}} = \int^t u_{\text{SNR}}(t') dt'$ is the SNR shock radius. The flow velocity of the downstream region of the SNR shock, $u_{2,\text{SNR}}$, is approximately given by $u_{2,\text{SNR}}(r, t) = (3u_{\text{SNR}}(t)/4 + V_w/4) (r/R_{\text{SNR}}(t))$. Here, the SNR shock is assumed to be the strong shock. The radius of the WTS, R_{WTS} , is fixed to be 8 pc because the velocity of the WTS is much smaller than the wind velocity and SNR shock velocity [8]. This WTS radius is almost consistent with the simulation of the evolution of the circumstellar medium [9]. The flow velocity of the downstream region of the WTS, $u_{2,\text{WTS}}$, is approximately given by $u_{2,\text{WTS}}(r) = (V_w/4)(r/R_{\text{WTS}})^{-2}$, where the WTS is assumed to be the strong shock.

In this work, we consider only the Parker-spiral magnetic field as an unperturbed magnetic field component in the free wind region (shock upstream region). To simplify, the magnetic field fluctuation and amplification in the free wind region are not considered in this work. The rotation axis of WR stars is set to be the polar axis of the spherical coordinate. θ and ϕ are polar angle and azimuthal angle, respectively. The poles and equator are the region where $\theta = 0, \pi$ and $\theta = \pi/2$, respectively. The Parker-spiral magnetic field, $\vec{B}_1 = B_{1,r}\vec{e}_r + B_{1,\phi}\vec{e}_\phi$, is

$$B_{1,r} = B_* \left(\frac{R_*}{r} \right)^2 \left\{ 1 - 2H \left(\theta - \frac{\pi}{2} \right) \right\}, \quad (2)$$

$$B_{1,\phi} = \mp B_* \frac{R_*}{r} \frac{R_* \Omega_*}{V_w} \sin \theta \left\{ 1 - 2H \left(\theta - \frac{\pi}{2} \right) \right\}, \quad (3)$$

where r is the distance from the explosion center [10]. The Alfvén radius, where the magnetic field opens, could be almost the same as the stellar radius under the WR star parameters we use in this work [11]. The sign of $B_{1,\phi}$ is negative (positive) when the angle between the rotation and magnetic axes, α_{inc} , is smaller (larger) than $\pi/2$ radians. We consider aligned rotators, which the rotation axis is parallel or antiparallel to the magnetic axis. The current sheet of aligned rotators is created at the equator [12]. The current sheet is assumed to be discontinuity in this work because the gyro radius of high-energy protons is assumed to be much larger than the width of the current sheet. The wind velocity is assumed to have only the radial component ($\vec{V}_w = V_w \vec{e}_r$). Thus, in the simulation frame (explosion center rest frame), the motional electric field, $\vec{E}_1 = -(\vec{V}_w/c) \times \vec{B}_1$, occurs in the free wind region. Contrary to the magnetic field in the free wind region (shock upstream region), the downstream magnetic field of both the SNR and WTS is assumed to be highly turbulent. The turbulent magnetic field in the shock downstream region is suggested from some observations and simulations [13, 14]. The particle motion in the downstream region of both the SNR and WTS is assumed to be the Bohm diffusion, which is suggested by some observations and simulations [15].

We use different methods to solve the particle transport in the upstream and downstream regions [4, 6, 16]. In the downstream region of both the SNR shock and WTS, we solve the random walk by using Monte-Carlo method. Downstream particles are isotropically scattered in the local downstream fluid rest frame. Scattering angle are randomly chosen between 0 and 4π steradians. The downstream particle mean free path is the downstream gyro radius because the Bohm diffusion is assumed in our simulations. The downstream magnetic field strength, which determines the downstream gyro radius, is given by the condition that some fractions of the upstream kinetic energy flux in the shock rest frame convert to the downstream magnetic energy flux. The conversion fraction, ϵ_B , is set to be 0.1 in our simulations. The magnetic field strength of the

downstream region of the SNR and WTS, $B_{2,\text{SNR}}$ and $B_{2,\text{WTS}}$, is

$$B_{2,\text{SNR}} = \sqrt{\frac{4\epsilon_B \dot{M} u_{\text{SNR}} - V_w}{V_w R_{\text{SNR}}}}, \quad (4)$$

$$B_{2,\text{WTS}} = \frac{\sqrt{4\epsilon_B \dot{M} V_w}}{R_{\text{WTS}}}, \quad (5)$$

respectively. On the other hand, in the free wind region (shock upstream region), we solve the equation of motion under \vec{B}_1 and \vec{E}_1 to solve the particle orbit.

3. Simulation results

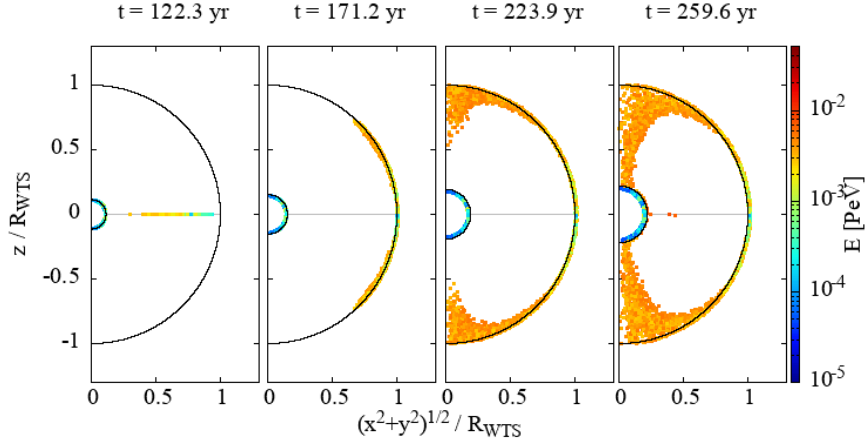


Figure 1: Time evolution of the particle distribution for a WR star with $\alpha_{\text{inc}} = 0$. The vertical axis is the z component of particle positions, which direction is parallel to the rotation axis of the progenitor. The horizontal axis is the distance from the rotation axis, $\sqrt{x^2 + y^2}$. The both axes are normalized by the radius of the WTS, R_{WTS} . The points and color are particles and the particle energy, respectively. The gray line at the equator ($z = 0$) is the current sheet. The inner and outer black hemispheres are the SNR shock and WTS, respectively. Time elapses from the left to right figures.

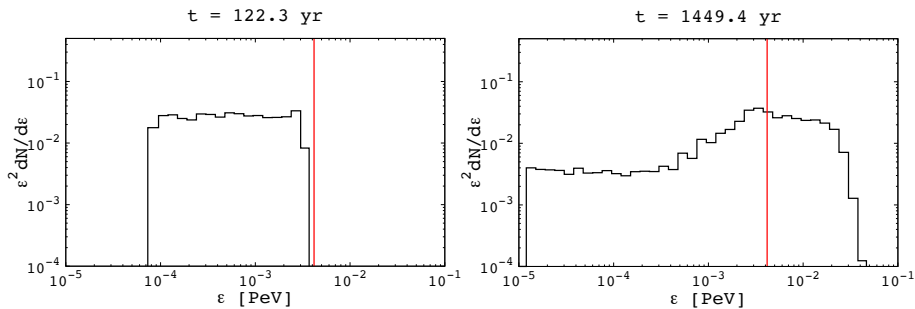


Figure 2: Energy spectrum of all particles at $t = 122.3$ yr and 1449.4 yr. The horizontal and vertical axes are the particle energy, ϵ , and $\epsilon^2 dN/d\epsilon$, respectively. The vertical red line is energy limited by escape from the SNR shock, ϵ_{SNR} (Equation (6)).

First, we show simulation results for the case of $\alpha_{\text{inc}} = 0$. Figure 1 shows the time evolution of the particle distribution for a WR star with $\alpha_{\text{inc}} = 0$. The vertical axis is the z component of particle positions, which direction is parallel to the rotation axis of progenitors. The horizontal axis is the distance from the rotation axis, $\sqrt{x^2 + y^2}$. The both axes are normalized by the radius of the WTS, R_{WTS} . The points and color are particles and the particle energy, respectively. The gray line at the equator ($z = 0$) is the current sheet. The inner and outer black hemispheres are the SNR shock and WTS, respectively. Time elapses from the left to right figures. Particles injected on the SNR shock surface are accelerated by the SNR shock while moving to the equator. Accelerating particles eventually reach the equator and interact with the current sheet at the equator. Once particles interact with the current sheet, these particles start to leave from the SNR shock while moving along the current sheet. The particle motion along the current sheet is the meandering motion [17]. This escape process from the SNR shock is the same as the results of our previous work [6]. Particles escaped from the SNR shock move along the current sheet towards the WTS ($t = 122.3$ yr in Figure 1). Once particles interact with the WTS, particles are accelerated by the WTS while moving along the WTS towards the poles ($t = 171.2$ yr in Figure 1). The radial magnetic field component, $B_{1,r}$, becomes larger than the toroidal magnetic field component, $B_{1,\phi}$ around the poles. Then, parallel shocks realize around the poles. Hence, particles around the poles can return to the SNR shock while moving the radial magnetic field component, $B_{1,r}$ ($t = 223.9$ yr in Figure 1). Particles returned to the SNR shock are accelerated again at the SNR shock. Particles move to the equator along the SNR shock and interact with the current sheet at the equator, leading to escape from the SNR shock again ($t = 259.6$ yr in Figure 1). Above cyclic motion between the SNR shock and WTS lasts until the SNR shock collides with the WTS ($t = 1449.4$ yr). Therefore, particles continue to be accelerated by the cyclic motion between the SNR shock and WTS.

Figure 2 shows the energy spectrum of all particles. The horizontal and vertical axes are the particle energy, ε , and $\varepsilon^2 dN/d\varepsilon$, respectively. The vertical red line is energy limited by escape from the SNR shock, ε_{SNR} , which is the same as the energy limited by the potential difference between the pole and equator [6]. The potential-limited maximum energy at the SNR, ε_{SNR} , is

$$\varepsilon_{\text{SNR}} = \frac{u_{\text{SNR}} - V_{\text{w}}}{c} \frac{R_* \Omega_*}{V_{\text{w}}} e B_* R_* . \quad (6)$$

At $t = 122.3$ yr, the maximum energy of particles is almost consistent with the potential-limited maximum energy (red line in Figure 2), which is the same as our previous work [6]. The energy spectrum of accelerated particles is almost same as the standard DSA prediction, $dN/d\varepsilon \propto \varepsilon^{-2}$ [2, 4]. As we mentioned above, particles can perform the cyclic motion between the SNR and WTS and are accelerated at both SNR and WTS again and again, leading to increasing the attainable maximum energy. Hence, as one can see, the attainable maximum energy can exceed the escape-limited maximum energy.

Next, we show results for the case of $\alpha_{\text{inc}} = \pi$. Figure 3 shows the time evolution of the particle distribution for a WR star with $\alpha_{\text{inc}} = \pi$. The horizontal and vertical axes, points, colors, inner and outer black hemispheres, and gray line at the equator ($z = 0$) are the same as Figure 1. Time elapses from the left to right figures. Contrary to the case of $\alpha_{\text{inc}} = 0$, injected particles move to the poles while being accelerated because the sign of toroidal magnetic field component, $B_{1,\phi}$, is opposite to that of the case of $\alpha_{\text{inc}} = 0$. The radial magnetic field component, $B_{1,r}$, is larger than the toroidal

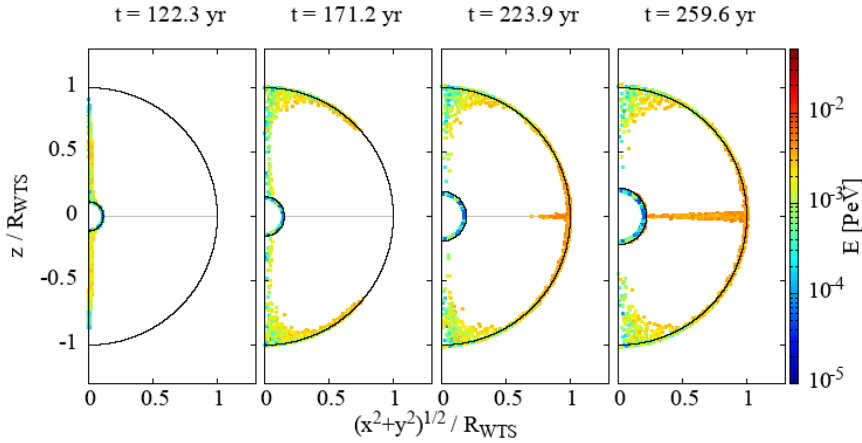


Figure 3: Time evolution of the particle distribution for a WR star with $\alpha_{\text{inc}} = \pi$. The horizontal and vertical axes, points, colors, inner and outer black hemispheres, and gray line at $z = 0$ are the same formats as Figure 1. Time elapses from the left to right figures.

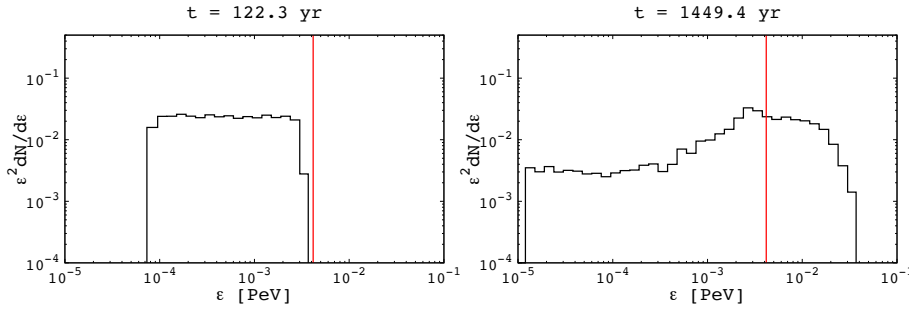


Figure 4: Energy spectra of all particles. The horizontal and vertical axes are the particle energy, ϵ , and $\epsilon^2 dN/d\epsilon$, respectively. The vertical red line is energy limited by escape from the SNR shock, ϵ_{SNR} (Equation (6)).

magnetic field component, $B_{1,\phi}$, around the poles. Therefore, particles around the poles can move along the radial magnetic field, $B_{1,r}$, and escape from the SNR shock while moving along the poles. This escape process from the SNR shock is the same as our previous work [6]. Particles escaped from the SNR shock move to the WTS and eventually reach the WTS ($t = 122.3$ yr in Figure 3). Particles are accelerated at the WTS while moving along the WTS ($t = 171.2$ yr in Figure 3). These particles reach the equator of the WTS and can return to the SNR shock while moving along the current sheet (meandering motion) ($t = 223.9 - 259.6$ yr in Figure 3). Particles are accelerated at the SNR shock again and escape from the poles again. This cyclic motion between the pole and equator occurs until the SNR shock collides with the WTS ($t = 1449.4$ yr) and particles continue to be accelerated by the cyclic motion between the SNR shock and WTS.

Figure 4 shows the energy spectrum of all particles. The horizontal and vertical axes are the particle energy, ϵ , and $\epsilon^2 dN/d\epsilon$, respectively. The vertical red line is energy limited by escape from the SNR shock, ϵ_{SNR} (Equation (6)). Similar to the case of $\alpha_{\text{inc}} = 0$, the maximum energy of particles escaped from the SNR shock is limited by the potential difference between the pole

and equator ($t = 122.3$ yr) [6]. The energy spectrum of accelerated particles is almost same as the standard DSA prediction, $dN/d\varepsilon \propto \varepsilon^{-2}$ [2, 4]. As we mentioned above, particles can experience the cyclic motion between the SNR shock and WTS until the SNR shock collides with the WTS ($t = 1449.4$ yr), leading to increasing the attainable maximum energy. Thus, the attainable maximum energy can exceed the potential-limited maximum energy similar to the case of $\alpha_{\text{inc}} = 0$.

4. Discussion

The spectral break of CR protons and heliums around 10 TeV is reported by some observations [1]. However, the origin of the spectral break around 10 TeV is still unclear. Our recent work showed that the maximum energy limited by escape from core-collapse SNRs without upstream magnetic field amplification is about 10 TeV [6]. As one can see Figures 2 and 4, the attainable maximum energy can reach 10 TeV by the cyclic motion between the SNR shock and WTS even if the escape-limited maximum energy (Equation (6)), is smaller than 10 TeV. Furthermore, our recent work showed that the perpendicular shock region of type Ia SNRs without upstream magnetic field amplification accelerate particles up to about 10 TeV [16]. Hence, SNRs without upstream magnetic field amplification could be the origin of the spectral break around 10 TeV.

5. Summary

In this work, we performed global test particle simulations to investigate the particle motion and attainable maximum energy of particles accelerated in core-collapse SNRs propagating in the free wind region. The Parker-spiral magnetic field, current sheet, and WTS in free wind region are considered in this work. For simplicity, the Parker-spiral magnetic field is only considered as the magnetic field in the free wind region (shock upstream region). The magnetic fluctuations in the upstream and downstream regions is assumed to be zero and highly amplified. We focus on WR stars, which are thought to be progenitors of type Ib/Ic supernovae. We show that particles can perform the cyclic motion between the equator and poles for both case of $\alpha_{\text{inc}} = 0$ and π and that the attainable maximum energy can exceed the maximum energy limited by the escape from the SNR shock (Equation (6)). Core-collapse SNRs without upstream magnetic field amplification could be the origin of the 10 TeV break of the CR energy spectrum.

Acknowledgments

We thank M. Hoshino and T. Amano for valuable comments. Numerical computations were carried out on Cray XC50 at Center for Computational Astrophysics, National Astronomical Observatory of Japan. This work is supported by JSPS KAKENHI grants JP19H01893 and No. JP21H04487.

References

- [1] Y. S. Yoon *et al.*, *Astrophys. J.* **839**, 5 (2017); E. Atkin *et al.*, *JETP Lett.* **108**, 5 (2018); Q. An *et al.* (DAMPE Collaboration), *Sci. Adv.* **5**, eaax3793 (2019); F. Alemanno *et al.* (DAMPE

- Collaboration), Phys. Rev. Lett. **126**, 201102 (2021); A. Albert *et al.* (HAWC Collaboration), Phys. Rev. D **105**, 063021 (2022).
- [2] G. F. Krymsky, Sov. Phys. Dokl. **23**, 327 (1977); W. I. Axford, E. Leer and G. Skadron, *Proceedings of the 15th International Cosmic Ray Conference* (1977), Vol. 11, p. 132; R. D. Blandford and J. P. Ostriker, Astrophys. J. **221**, L29 (1978); A. R. Bell, Mon. Not. R. Astron. Soc. **182**, 147 (1978).
- [3] R. B. Decker and L. Vlahos, Astrophys. J. **306**, 710 (1986); J. Giacalone, Astrophys. J. **624**, 765 (2005); F. Guo and J. Giacalone, Astrophys. J. **715**, 406 (2010).
- [4] S. F. Kamijima, Y. Ohira, and R. Yamazaki, Astrophys. J. **897**, 116 (2020).
- [5] V. S. Ptuskin and V. N. Zirakashvili, Astron. Astrophys. **403**, 1 (2003); **429**, 755 (2005); Y. Ohira, K. Murase, and R. Yamazaki, Astron. Astrophys. **513**, A17 (2010).
- [6] S. F. Kamijima and Y. Ohira, Phys. Rev. D **106**, 123025 (2022).
- [7] R. A. Chevalier, Astrophys. J. **258**, 790 (1982); T. J. Moriya, K. Maeda, F. Taddia, J. Sollerman, S. I. Blinnikov, and E. I. Sorokina, Mon. Not. R. Astron. Soc. **435**, 1520 (2013).
- [8] R. Weaver, R. McCray, J. Castor, P. Shapiro, and R. Moore, Astrophys. J. **218**, 377 (1977).
- [9] V. V. Dwarkadas, Astrophys. J. **667**, 226 (2007).
- [10] E. J. Weber and L. Davis Jr., Astrophys. J. **148**, 217 (1967).
- [11] A. ud-Doula, S. P. Owocki, and R. H. D. Townsend, Mon. Not. R. Astron. Soc. **385**, 97 (2008).
- [12] K. Alanko-Huotari, I. G. Usoskin, K. Mursula, and G. A. Kovaltsov, J. Geophys. Res. **112**, A08101 (2007); R. D. Strauss, M. S. Potgieter, I. Büsching, and A. Kopp, Astrophys. Space Sci. **339**, 223 (2012).
- [13] J. Giacalone and J. R. Jokipii, Astrophys. J. Lett. **663**, L41 (2007); T. Inoue, R. Yamazaki, and S. Inutsuka, Astrophys. J. **695**, 825 (2009); Y. Ohira, Astrophys. J. **817**, 137 (2016).
- [14] E. G. Berezhko, L. T. Ksenofontov, and H. J. Völk, Astron. Astrophys. **412**, L11 (2003); A. Bamba, R. Yamazaki and J. S. Hiraga, Astrophys. J. **632**, 294 (2005); Y. Uchiyama *et al.*, Nature (London) **449**, 576 (2007).
- [15] N. Tsuji, Y. Uchiyama, D. Khangulyan, and F. Aharonian, Astrophys. J. **907**, 117 (2021); M. D. Stage, G. E. Allen, J. C. Houck, and J. E. Davis, Nature Physics. **2**, 614 (2006); M. Hussein, and A. Shalchi, Astrophys. J. **785**, 31 (2014).
- [16] S. F. Kamijima and Y. Ohira, Phys. Rev. D **104**, 083028 (2021).
- [17] E. H. Levy, *14th International Cosmic Ray Conference Munich* (1975), Vol. 4, p. 1215; E. H. Levy, Nature (London) **261**, 394 (1976).